JOURNAL OF GEOPHYSICAL RESEARCH, VOL. 95, NO. B10, PAGES 15,853–15,858, SEPTEMBER 10, 1990

Reversals of the Orthoenstatite-Clinoenstatite Transition at High Pressures and High Temperatures

R. E. G. PACALO AND T. GASPARIK

Mineral Physics Institute, Department of Earth and Space Sciences
State University of New York at Stony Brook

The $MgSiO_3$ orthoenstatite-clinoenstatite (OEn-CEn) phase boundary has been reversed between pressures of 70 and 110 kbar and temperatures of 900°C and 1700°C with a split-sphere anvil apparatus (USSA-2000). Starting materials contained PbO-PbF_2 (1:1) flux to promote equilibration of the charges and eliminate a potential effect of deviatoric stresses on the phase boundary. The phase boundary separating orthoenstatite from clinoenstatite at high pressures and temperatures can be described by the equation P (kbar) = 0.031 T (°C) + 50. Our results are consistent with previous unreversed determinations of the boundary at these high-pressure, high-temperature conditions. However, the dP/dT slope determined in the present study is much smaller than that implied by earlier experimental studies of the orthoenstatite/low clinoenstatite boundary at low pressures and temperatures. We propose that the clinoenstatite observed at high pressures and temperatures is a new high-pressure clinoenstatite phase which is possibly an analogue of $MgGeO_3$ clinopyroxene.

INTRODUCTION

The stability of the $MgSiO_3$ polymorphs has been under investigation for many years. Terrestrial rocks contain almost exclusively orthoenstatite (OEn-Pbca), while clinoenstatite (CEn-$P2_1/c$) is often found in meteorites [see *Reid and Cohen*, 1967, and references therein]. The first observation of a multiply twinned terrestrial clinoenstatite was documented by *Dallwitz et al.* [1966]. Subsequent workers have found clinoenstatite-bearing rocks in association with ophiolite complexes [e.g., *Komatsu*, 1980; *Sameshima et al.*, 1983]. Based on the experimental work of *Atlas* [1952] and *Boyd and Schairer* [1964], these naturally occurring clinoenstatites were interpreted as a metastable low-temperature phase resulting from rapid cooling of the low-pressure, high-temperature polymorph, protoenstatite (PEn-Pbcn). However, later phase equilibrium experiments [*Sclar et al.*, 1964; *Boyd and England*, 1965] appeared to support the existence of a stable clinoenstatite at low temperatures, although their orthoenstatite-clinoenstatite boundaries differed somewhat in pressure and temperature (Figure 1).

The observation of untwinned clinoenstatite within kink bands of bronzite crystals [*Trommsdorff and Wenk*, 1968] represented an additional occurrence of terrestrial clinoenstatite. The extreme bending and kinking of bronzite was indicative of the intense deformation experienced by the host gabbro. Orthoenstatite was known to invert to clinoenstatite at temperatures both above and below the experimentally determined boundary when shear stresses were applied [*Riecker and Rooney*, 1967], and the isomorphous pyroxene ferrosilite ($FeSiO_3$) also experienced an orthohombic to monoclinic inversion under shearing conditions [*Lindsley and Munoz*, 1969]. This raised the possibility that the occurrences of clinoenstatite in nature were metastable, resulting from the stress-induced inversion of orthopyroxene rather than representing stable occurrences.

The recognition that nonhydrostatic stresses can affect the location of the equilibrium orthoenstatite-clinoenstatite boundary and the discrepancy between the boundaries determined by *Sclar et al.* [1964] and *Boyd and England* [1965] cast some doubt on the true existence of a low-temperature clinoenstatite stability field. *Grover* [1972*a*, *b*] resolved this issue by reversing the orthoenstatite-clinoenstatite boundary in hydrothermal pressure vessels at 2 and 4 kbar and 450°C–750°C, thus proving the stability of clinoenstatite at low temperatures. Molten chloride salts ($MgCl_2 \cdot H_2O$) were used as fluxes to enhance the extremely sluggish transformation rates (1–2 months) and to ensure hydrostatic conditions. Grover's boundary is qualitatively similar to those determined in the earlier phase equilibria studies, although his dP/dT slope is not as steep as previously indicated (Figure 1). The discrepancy between the studies of *Sclar et al.* [1964] and *Boyd and England* [1965] has since been partly attributed to the differences in their experimental techniques. Specifically, the differences in the nonhydrostatic stress regimes between the belt or girdle [*Sclar et al.*, 1964] and the piston-cylinder [*Boyd and England*, 1965] pressure devices, as well as their respective choices of oxide or crystalline starting materials may have contributed to the differences in the phase boundary location [*Grover*, 1972*b*].

The $MgSiO_3$ phase relations are further complicated by the observation of an orthoenstatite-clinoenstatite transition at high pressures and temperatures [*Yamamoto and Akimoto*, 1977; M. Kanzaki, personal communication, 1988]. This boundary has a much larger pressure dependence than the orthoenstatite/low clinoenstatite boundary determined by *Grover* [1972*a*, *b*]. Experimental data for the orthoferrosilite-clinoferrosilite transition show a similar discrepancy between the results of *Lindsley* [1965] and *Akimoto et al.* [1965]. The current understanding of phase relations in both the $MgSiO_3$ and $FeSiO_3$ systems is summarized in Figure 1.

The high-pressure, high-temperature orthoenstatite-clinoenstatite boundaries of *Yamamoto and Akimoto* [1977] and M. Kanzaki are very similar (Figure 1). The boundary of *Yamamoto and Akimoto* [1977] was determined by synthesis experiments, while M. Kanzaki (personal communication, 1988) did achieve a reversal at 1300°C using a mix of orthoenstatite and clinoenstatite; at other temperatures the starting material was $MgSiO_3$ glass. In both studies, the cell

Paper number 90JB00302.
0148-0227/90/90JB-00302$05.00

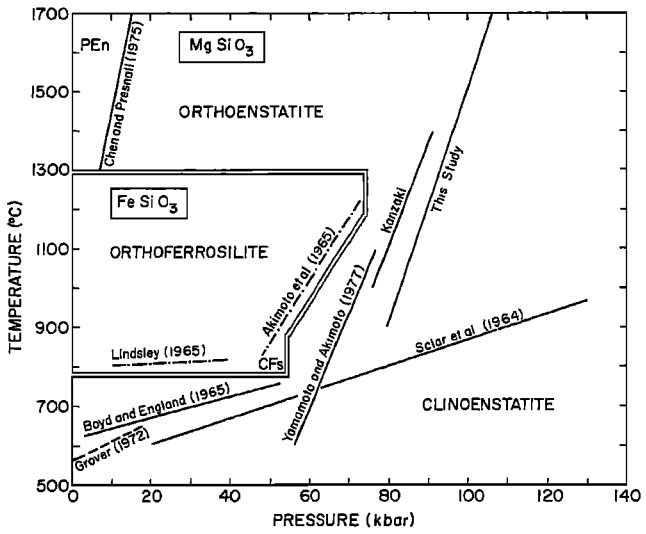

Fig. 1. A summary of the experimental observations in the systems $MgSiO_3$ and $FeSiO_3$.

assemblies were calibrated at room temperature. Thus the sample pressures may have been underestimated at high temperatures due to a potential increase in the efficiency of the cell assembly with increasing temperature.

This study was undertaken in an attempt to clarify the equilibrium phase relations between orthoenstatite and clinoenstatite, and particularly the discrepancy in the slope of the orthoenstatite-clinoenstatite transition, by obtaining reversals under hydrostatic conditions at high pressures and temperatures.

EXPERIMENTAL TECHNIQUES

The high-pressure experiments reported in this paper were carried out with a uniaxial split-sphere anvil apparatus (USSA-2000). The press consists of a two-stage anvil system that is capable of reaching simultaneously high pressures and high temperatures (in excess of 200 kbar and 2000°C). The first-stage anvils form a steel sphere divided into six parts; these anvils are permanently mounted into a stationary upper and a movable lower guide block. The second stage, consisting of eight tungsten carbide cubes, each truncated on an inner corner, is placed in the cubic cavity formed by the first-stage anvils. When assembled, the truncations form an octahedral cavity that holds the sample assembly. The entire unit is compressed by a 2000-t uniaxial hydraulic press. The cell assembly used in the present study was a semisintered MgO octahedron with a 10-mm edge length. A cylindrical sleeve of $LaCrO_3$ was used as a heater. The sample material was placed in a platinum capsule welded at one end and crimped at the other. On average, the capsule volume started at 4 mm^3 (3 mm long × 1.3 mm diameter) and was reduced to 2.3 mm^3 (2 mm long × 1.2 mm diameter) after an experiment. A detailed description of the split-sphere apparatus, sample assembly, and experimental procedures is given by *Gasparik* [1989].

The sample temperature was measured by a W3%Re/W25%Re thermocouple directly in contact with the platinum capsule. A Eurotherm controller held the nominal temperature to within 5°C of the set point, and any fluctuations were generally too rapid to have any effect on the sample. No

TABLE 1. Compositions of Starting Materials

Starting Material	Composition, mol
En-1	1.00 MgO, 1.20 SiO_2, 0.10 PbO, 0.10 PbF_2
En-3	1.00 MgO, 1.10 SiO_2, 0.05 PbO, 0.05 PbF_2
W	En-1 + 5 wt % OEn seeds
X	En-1 + 5 wt % OEn + 5 wt % CEn seeds
Y	En-3 + 5 wt % OEn seeds

corrections for the effect of pressure on the thermocouple emf were applied. The hotspot in the sample capsule was located approximately 0.7 mm from the thermocouple end. Using two-pyroxene thermometry, *Gasparik* [1989] has estimated the temperature distribution in the sample. The temperature measured and controlled by the thermocouple is approximately in the center of the sample. The temperature increases by about 50°C between the center of the cell and the hotspot; the temperature drop between the hotspot and the cold end of the capsule is approximately 200°C. The reproducibility of the experimental temperatures is estimated at ±30°C.

The sample pressures were calibrated against the gauge pressures at room temperature by monitoring pressure-induced resistance changes in metals [*Gasparik*, 1989]. At high temperature, the calibration is based on reversals of the coesite-stishovite boundary, which was determined by *Yagi and Akimoto* [1976] and is described by

$$P\ (\text{kbar}) = 0.011T(°\text{C}) + 80.$$

The starting material for these calibration runs was amorphous silica with 10 wt % each of coesite and stishovite. Run conditions for the SiO_2 reversals are summarized in Table 2. Sample pressures were reproducible to within 3 kbar.

Starting materials for the orthoenstatite-clinoenstatite reversals were mechanical mixes of high purity MgO, SiO_2, PbO, and PbF_2 (Table 1). The PbO-PbF_2 flux was added in order to eliminate potential deviatoric stresses arising from the use of the solid pressure-transmitting medium, to minimize pressure gradients within the sample, and to promote equilibration. This flux was chosen because of the low melting point of its 1:1 molar ratio mix. The molar ratio of enstatite mix to flux was either 10:1 or 20:1. The higher-temperature experiments required less flux to produce a similar degree of melting. In each case, excess silica was added to combine with the flux and to preclude the formation of forsterite (Mg_2SiO_4). Microprobe analyses (WDS or EDS) failed to detect any lead in the pyroxene run products. In addition, the analysis weight totals were 100%, rendering the presence of fluorine unlikely.

Approximately 5 wt % of large seed crystals of orthoenstatite or clinoenstatite were added to each oxide mix to eliminate potential problems with nucleation and to ensure that large crystals suitable for optical identification were present in the run products. Orthoenstatite seeds up to 100 μm in length were grown from a stoichiometric oxide mix at 60 kbar and 1400°C. The same mix was used to grow clinoenstatite seeds (inverted protoenstatite) at 1300°C and 1 atm pressure. These seeds were subsequently annealed at 800°C and 1 atm to increase the grain size; their average length was 20–50 μm. The seed pyroxenes were identified by powder X ray diffractometry and optical microscopy. Start-

TABLE 2. Experimental Conditions and Results

Run	P_{ram}, bars	P_{sample}, kbar	T, °C	Starting Material	End Product[a]	Comments
				OEn-CEn		
62	320	142	1200	W[b]	CEn	
141	160	100	1300	W	CEn	
144	110	77	1300	W	CEn	
154	130	87	1300	W	OEn	
161	145	94	1300	W	CEn	
195	120	82	1100	W	OEn	
198	130	87	1100	W	CEn	
202	86	64	900	W	OEn+CEn	no melt
204	125	85	1100	W	CEn	
210	93	68	950	W	OEn	no reaction
214	170	103	1700	Y	OEn	
216	102	73	950	W	OEn	no reaction
221	180	107	1700	Y	CEn	
227	110	77	950	W	OEn	no reaction
228	102	73	900	W[c]	OEn	no reaction
251	120	82	950	W	CEn	
291	110	77	1000	X	OEn	
301	120	82	1000	X	CEn	
318	150	96	1500	X	OEn+CEn	phase boundary in the sample
				Cs-St		
385	142	92	1200	Z[d]	Cs+St	phase boundary in the sample
438	150	96	1400	Z	Cs+St	phase boundary in the sample

[a]CEn, clinoenstatite crystals ± matrix and glass; OEn, orthoenstatite crystals ± matrix and glass.
[b]Starting compositions given in Table 1.
[c]$MgCl_2 \cdot 6H_2O$ added as extra flux.
[d]Z = 10 wt % Cs seeds + 10 wt % St seeds + amorphous silica.

ing material W contained orthoenstatite seed crystals in a matrix of oxide mix En-1. Starting material X contained large clinoenstatite seeds in a matrix of En-1. Additionally, 5 wt % of finely ground orthoenstatite powder was added to this starting material to overcome difficulties with orthoenstatite nucleation. The oxide mix En-3 was used as a matrix for starting material Y, which also contained large orthoenstatite seeds. This starting material was more appropriate at high temperatures (1700°C) because it contained proportionally less flux.

Experimental charges, still within their platinum capsules, were mounted in epoxy. Longitudinal thin sections were made from each mount and observed under an optical microscope. The experimental products were identified by extinction angle, birefringence, and grain size. The orthoenstatite crystals exhibited parallel extinction and had low birefringence; generally, these crystals grew to large sizes and were euhedral or subhedral. The clinoenstatite crystals showed angular extinction and higher birefringence and were often polysynthetically twinned. They were generally smaller and more irregular than the rhombic form. In most experiments long slender quench crystals formed in the cold or bottom end of the capsule. Located just below the quench crystals was a layer of highly birefringent flux crystals which separated out from the melt due to gravity.

RESULTS

The experimental conditions and results are listed in Table 2. All experiments were 6 hours in duration. The starting materials with orthoenstatite seeds (W and Y) were used for most of the experiments. Half brackets were obtained by equilibrating these starting materials in the clinoenstatite stability field. Clinoenstatite crystals formed from the original orthoenstatite seeds could easily be identified by their larger size in contrast to the fine matrix. When these starting materials were held within the orthoenstatite stability field, the resultant sample consisted entirely of large orthoenstatite crystals. Thus the original orthoenstatite seed crystals grew at the expense of the matrix, indicating the stability of orthoenstatite.

At temperatures below 1100°C the reaction rates were slow. Run 202, at 900°C, probably did not produce melt; the sample appeared to contain some clinoenstatite, but presumably, deviatoric stresses were present. A small amount (~0.5 mm^3) of additional flux material, $MgCl_2 \cdot 6H_2O$, was added to run 228 to produce melt at this low temperature. Melting did occur, but the orthoenstatite seed crystals appeared unaltered, suggesting either that orthoenstatite was stable or that the reaction did not occur. Melting occurred at 950°C in runs 210, 216, and 227, but the orthoenstatite seed crystals were still clearly orthorhombic in these run products. However, clinoenstatite crystals formed from orthoenstatite seeds in the presence of melt at 82 kbar and 950°C (run 251), producing a reversal at these conditions.

Starting material X, made of both fine orthoenstatite powder and large clinoenstatite seeds, was used to obtain half brackets on the low-pressure side of the boundary. Run 301 within the clinoenstatite field did not produce any observable changes in the clinoenstatite starting seeds, indicating no reaction. On the other hand, the experiments within the orthoenstatite stability field (runs 291 and 318) produced large orthoenstatite crystals (100–500 μm in length) which grew from the original clinoenstatite seeds and the fine matrix.

The product from run 318 (96 kbar, 1500°C) contained the orthoenstatite-clinoenstatite boundary, which was located

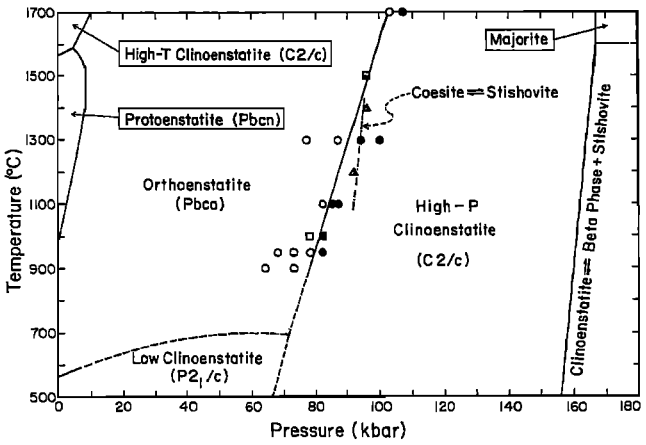

Fig. 2. Temperature-pressure phase diagram for the $MgSiO_3$ system showing the location of the present experiments. Circles correspond to experiments with the starting materials W and Y. Squares denote results with the starting material X. Open symbols represent orthoenstatite run products, while solid symbols indicate clinoenstatite products. The triangles represent reversals of the coesite-stishovite boundary. The dash-dot line is the boundary of *Yagi and Akimoto* [1976]. Extrapolations of the experimentally determined boundaries are dashed. The high-T clinoenstatite and protoenstatite stability fields are calculated from the thermodynamic model of *Gasparik* [1990].

approximately in the center of the capsule. Large subhedral orthoenstatite crystals were present in the hotter half of the sample where temperatures ranged from 1500° to 1550°C. The colder end, at temperatures between 1350° and 1500°C, contained a very fine matrix, presumably clinoenstatite, similar in appearance to that found in run 301, with no clearly identifiable crystals. The presence of this boundary is undoubtedly a consequence of the longitudinal temperature gradient within the sample assembly. The orthoenstatite-clinoenstatite boundary was also observed by *Presnall and Gasparik* [1989] at 116 kbar and 2140°C with the same sample assembly. Their boundary separated a single-crystal of orthoenstatite in the hot end of the sample from an aggregate of clinoenstatite crystals in the cold end. Melting occurred in the hotspot.

Figure 2 presents a summary of the data from the present study. The boundary between orthoenstatite and clinoenstatite, which best fits the data from the present study and the data of *Presnall and Gasparik* [1989], is given by

$$P\ (\text{kbar}) = 0.031T(°\text{C}) + 50.$$

Discussion

The following summarize the present understanding of orthoenstatite and clinoenstatite stability:

1. *Grover* [1972*a*, *b*] produced hydrostatic reversals of the orthoenstatite/low clinoenstatite (Pbca-$P2_1/c$) phase boundary at 2 and 4 kbar pressures and temperatures between 450° and 750°C. The slope of this boundary is 222 bar K^{-1}.

2. In the present study and the study of *Presnall and Gasparik* [1989], hydrostatic reversals of the orthoenstatite-clinoenstatite boundary were obtained at pressures between 70 and 116 kbar and temperatures between 900° and 2140°C. The results indicate a straight boundary with the slope of 31 bars K^{-1}.

The slopes of the orthoenstatite-clinoenstatite boundaries determined in Grover's study and in the present study are very different. It seems unlikely that the clinoenstatite at both boundaries is the same phase, despite the fact that the quench products are identical (M. Kanzaki, personal communication, 1988). *Yamamoto and Akimoto* [1977] located the orthoenstatite-clinoenstatite boundary to very low temperatures and reported orthoenstatite stable even at temperatures as low as 625°C at 55 kbar. A linear extrapolation of the boundary determined by Grover would limit the stability of orthoenstatite to much higher temperatures. To satisfy the observations of *Yamamoto and Akimoto* [1977], the orthoenstatite/low clinoenstatite boundary must curve to lower temperatures at higher pressures, in the opposite sense than would be required if the clinoenstatite at both boundaries were the same phase. Thus either *Grover*'s [1972*a*, *b*] data are incorrect or the clinoenstatite phase observed at high pressures and temperatures is not low clinoenstatite but is a new phase, high-pressure (high-P) clinoenstatite.

Another argument against the stability of low clinoenstatite at high pressures and temperatures, and in favor of Grover's results, is the small volume change associated with the orthoenstatite/low clinoenstatite transition [*Stephenson et al.*, 1966]. If this small ΔV is combined with the small slope of the boundary determined in the present study, an entropy of transition of the order of 10^{-2} J mol^{-1} K^{-1} would be required. Any small differences between orthoenstatite and clinoenstatite in higher-order properties such as compressibility, thermal expansion, or heat capacity would produce a curvature in the phase boundary. However, the tightly constrained boundary between orthoenstatite and high-P clinoenstatite extends over a 1300°C temperature interval without any obvious curvature. Thus, the initial assumption of a small ΔV for the orthoenstatite/high-P clinoenstatite transition is unlikely to be correct. This is supported by the distinct kink observed on the enstatite melting curve of *Presnall and Gasparik* [1989], which is suggestive of a large volume change for the orthoenstatite/high-P clinoenstatite transition.

The orthopyroxene-clinopyroxene (Pbca-C2/c) transition in the $MgGeO_3$ system has a large volume change of -1.17 cm^3 mol^{-1} [*Ross and Navrotsky*, 1988]. Germanates are often used as silicate analogues because they experience transformations similar to silicates but at lower pressures. The $MgGeO_3$ orthopyroxene-clinopyroxene transition was calculated by *Ross and Navrotsky* [1988] using several different thermochemical data sets. The locations of boundaries calculated from different data sets were all in good agreement. The germanate transition is not a good analogue for the orthoenstatite-low clinoenstatite transition; not only are the clinopyroxene structures different (i.e., low clinoenstatite belongs to space group $P2_1/c$, whereas $MgGeO_3$ clinopyroxene belongs to C2/c) but also the enthalpy, entropy, and volume changes associated with this transition in the $MgGeO_3$ system are much larger than the corresponding parameters for the orthoenstatite/low clinoenstatite transition. However, the transition in the germanate pyroxene appears to be a very good analogue for the orthoenstatite/high-P clinoenstatite transition. Besides the large volume change inferred for the $MgSiO_3$ transition, the dP/dT slopes are very similar, 21 bars K^{-1} calculated for $MgGeO_3$ com-

pared to 31 bars K^{-1} determined in the present study. By analogy, the nonquenchable high-P clinoenstatite is expected to crystallize in the space group C2/c.

Because the volume change for the orthoenstatite/high-P clinoenstatite transition is predicted to be large, the location of this phase boundary is not likely to be affected by slight deviatoric stresses within the sample. Thus the initial requirement for a hydrostatic pressure environment is not so critical to the determination of the high-P clinoenstatite stability field. However, the presence of deviatoric stresses probably did contribute to the shift in the position of the orthoenstatite/low clinoenstatite boundary between the studies of *Sclar et al.* [1964] and *Boyd and England* [1965] and the work of *Grover* [1972*a*, *b*], although these deviatoric stresses can not be responsible for the observed differences in the boundary's slope [*Coe*, 1970]. The boundaries of *Sclar et al.* [1964] and *Boyd and England* [1965] were determined at higher pressures than *Grover*'s [1972*a*, *b*] boundary. Their steeper *dP/dT* slopes most probably reflect the projected curvature of the low-pressure boundary defined by Grover.

At 1 atm and high temperature, *Perrotta and Stephenson* [1965] observed a transformation from low clinoenstatite to a new high-temperature pyroxene phase; they named the new phase high clinoenstatite. *Smith* [1969] suggested that high clinoenstatite has a C2/c structure. This reversible metastable transition from low clinoenstatite to high clinoenstatite at 1 atm and 995°C was also observed by *Sharma et al.* [1987] with high-temperature Raman spectroscopy. A similar nonquenchable transition also occurs in iron-bearing pyroxene compositions but at lower temperatures [*Grover*, 1972*b*; *Smyth*, 1974]. The high (T) clinoenstatite is most likely an end-member of the enstatite-diopside (C2/c) clinopyroxene solution used in thermodynamic models for calculating the phase relations on the enstatite-diopside join. Experimental data on the enstatite-diopside join predict the stability of the high (T) clinoenstatite at higher temperatures and lower pressures than the stability field of orthoenstatite [e.g., *Lindsley et al.*, 1981]. However, the high-P clinoenstatite is stable at lower temperatures and higher pressures than orthoenstatite. The experimentally observed phase relations on the enstatite-diopside join can not be reproduced by using the presently determined boundary as the orthoenstatite-clinoenstatite reaction. Thus the high-P clinoenstatite appears to be a C2/c polymorph different from the high (T) clinoenstatite of the (C2/c) enstatite-diopside solution.

The orthoenstatite/high-P clinoenstatite boundary determined in this study occurs at slightly higher pressures than the boundaries reported by either *Yamamoto and Akimoto* [1977] or M. Kanzaki (personal communication, 1988). As discussed previously, several possible reasons for this discrepancy exist. First, this work consists of carefully controlled reversals of the boundary, whereas the majority of data from the earlier studies were obtained from synthesis experiments. Second, differences in the pressure calibration techniques could easily produce small offsets in the pressure scale. For instance, the high-pressure assembly is often more efficient at high temperatures. Therefore pressure calibrations done at room temperature, as in the earlier studies, could systematically underestimate sample pressures in the high-temperature experiments. In this study, the calibration experiments determined precisely the position of the orthoenstatite/high-P clinoenstatite boundary relative to the coesite-stishovite boundary, which is one of the best known calibration curves at high pressures.

CONCLUSIONS

The phase boundary separating orthoenstatite from clinoenstatite at high pressures and temperatures has been determined over a temperature interval of 1300°C and can be described by

$$P\ (\text{kbar}) = 0.031T(^\circ\text{C}) + 50.$$

Our reversed boundary is in agreement with the earlier determinations. The *dP/dT* slope obtained in the present study is much smaller than the slope of the orthoenstatite/low clinoenstatite transition at much lower pressures and temperatures. It is suggested that the clinoenstatite phase stable at high pressures and temperatures is a new high-pressure polymorph of $MgSiO_3$, different from low or high (T) clinoenstatite. The $MgGeO_3$ orthopyroxene-clinopyroxene (Pbca-C2/c) transition appears to be a good analogue for the orthoenstatite/high-P clinoenstatite transition. Based on the similarities between these systems, the volume change for the orthoenstatite/high-P clinoenstatite transition is expected to be close to the volume change for the corresponding transition in $MgGeO_3$, and the space group of the new high-pressure phase is predicted to be C2/c. The high-P clinoenstatite phase is not quenchable, so in situ confirmation of the space group is needed.

Acknowledgments. This study was supported by a National Science Foundation grant EAR 86-17550 to T. Gasparik. The high-pressure experiments reported in this paper were performed in the Stony Brook High Pressure Laboratory which is jointly supported by the National Science Foundation Division of Earth Sciences (EAR 86-07105) and the State University of New York at Stony Brook.

REFERENCES

Akimoto, S., T. Katsura, Y. Syono, H. Fujisawa, and E. Komada, Polymorphic transition of pyroxenes $FeSiO_3$ and $CoSiO_3$ at high pressures and temperatures, *J. Geophys. Res.*, *70*, 5269–5278, 1965.

Atlas, L., The polymorphism of $MgSiO_3$ and solid-state equilibria in the system $MgSiO_3$-$CaMgSi_2O_6$, *J. Geol.*, *60*, 125–147, 1952.

Boyd, F. R., and J. L. England, The rhombic enstatite-clinoenstatite inversion, *Year Book Carnegie Inst. Washington*, *64*, 117–120, 1965.

Boyd, F. R., and J. F. Schairer, The system $MgSiO_3$-$CaMgSi_2O_6$, *J. Petrol.*, *5*, 275–309, 1964.

Chen, C.-H., and D. C. Presnall, The system Mg_2SiO_4-SiO_2 at pressures up to 25 kilobars, *Am. Mineral.*, *60*, 398–406, 1975.

Coe, R. S., The thermodynamic effect of shear stress on the ortho-clino inversion in enstatite and other coherent phase transitions characterized by a finite simple shear, *Contrib. Mineral. Petrol.*, *26*, 247–264, 1970.

Dallwitz, W. B., D. H. Green, and J. E. Thompson, Clinoenstatite in a volcanic rock from the Cape Vogel area, Papua, *J. Petrol.*, *7*, 375–403, 1966.

Gasparik, T., Transformation of enstatite-diopside-jadeite pyroxenes to garnet, *Contrib. Mineral. Petrol.*, *102*, 389–405, 1989.

Gasparik, T., A thermodynamic model for the estatite-diopside join, *Am. Mineral.*, in press, 1990.

Grover, J., The stability of low-clinoenstatite in the system $Mg_2Si_2O_6$-$CaMgSi_2O_6$ (abstract), *Eos Trans. AGU*, *53*, 539, 1972*a*.

Grover, J. Two problems in pyroxene mineralogy, Ph.D. thesis, 181 pp., Yale Univ., New Haven, Conn., 1972*b*.

Komatsu, M., Clinoenstatite in volcanic rocks from the Bonin Islands, *Contrib. Mineral. Petrol.*, *74*, 329–338, 1980.

Lindsley, D. H., Ferrosilite, *Year Book Carnegie Inst. Washington*, *64*, 148–150, 1965.

Lindsley, D. H., and J. L. Munoz, Ortho-clino inversion in ferrosilite, *Year Book Carnegie Inst. Washington*, *67*, 86–88, 1969.

Lindsley, D. H., J. E. Grover, and P. M. Davidson, The thermodynamics of the $Mg_2Si_2O_6$-$CaMgSi_2O_6$ join: A review and an improved model, in *Thermodynamics of Minerals and Melts*, edited by R. C. Newton, A. Navrotsky, and B. J. Wood, pp. 149–175, Springer-Verlag, New York, 1981.

Perrotta, A. J., and D. A. Stephenson, Clinoenstatite: High-low inversion, *Science*, *148*, 1090–1091, 1965.

Presnall, D. C., and T. Gasparik, Melting of enstatite from 10 to 16.5 GPa (abstract), *Eos Trans. AGU*, *70*, 508, 1989.

Reid, A. M., and A. J. Cohen, Some characteristics of enstatite from enstatite achondrites, *Geochim. Cosmochim. Acta*, *31*, 661–672, 1967.

Riecker, R. E., and T. P. Rooney, Deformation and polymorphism of enstatite under shear stress, *Geol. Soc. Am. Bull.*, *78*, 1045–1054, 1967.

Ross, N. L., and A. Navrotsky, A calorimetric, spectroscopic, and phase equilibrium study of the $MgGeO_3$ polymorphs (orthopyroxene, clinopyroxene, and ilmenite structures), *Am. Mineral.*, *73*, 1355–1365, 1988.

Sameshima, T., J.-P. Paris, P. M. Black, and R. F. Heming, Clinoenstatite-bearing lava from Népoui, New Caledonia, *Am. Mineral.*, *68*, 1076–1082, 1983.

Sclar, C. B., L. C. Carrison, and C. M. Schwartz, High pressure stability fields of clinoenstatite, and the orthoenstatite-clinoenstatite transition (abstract), *Eos Trans. AGU*, *45*, 121 1964.

Sharma, S. K., S. Ghose, and J. P. Urmos, Raman study of high-temperature phase transitions in ortho- and clinoenstatite, (abstract), *Eos Trans. AGU*, *68*, 433, 1987.

Smith, J. V., Magnesium pyroxene at high temperature: Inversion in clinoenstatite, *Nature*, *222*, 256–257, 1969.

Smyth, J. R., The high temperature crystal chemistry of clinohypersthene, *Am. Mineral.*, *59*, 1069–1082, 1974.

Stephenson, C. A., C. B. Sclar, and J. V. Smith, Unit cell volumes of synthetic orthoenstatite and low clinoenstatite, *Mineral. Mag.*, *35*, 838–846, 1966.

Trommsdorff, V., and H.-R. Wenk, Terrestrial metamorphic clinoenstatite in kinks of bronzite crystals, *Contrib. Mineral. Petrol.*, *19*, 158–168, 1968.

Yagi, T., and S. Akimoto, Direct determination of coesite-stishovite transition by in-situ x-ray measurements, *Tectonophysics*, *35*, 259–270, 1976.

Yamamoto, K., and S. Akimoto, The system MgO-SiO_2-H_2O at high pressures and temperatures-stability field for hydroxyl-chondrodite, hydroxyl-clinohumite, and 10 Å-phase, *Am. J. Sci.*, *277*, 288–312, 1977.

T. Gasparik and R. E. G. Pacalo, Department of Earth and Space Sciences, State University of New York at Stony Brook, Stony Brook, NY 11794.

(Received June 29, 1989;
revised November 22, 1989;
accepted December 18, 1989.)